IN-VENTO 2014
XIII Conference of the Italian Association for Wind Engineering
22-25 June 2014, Genova, Italy

Evaluation of the thermal comfort by natural ventilation in hot climates

J. A. Castillo[1,2], G. Huelsz[1], T. van Hooff[2] and B. Blocken[2,3]

[1]Instituto de Energías Renovables, Universidad Nacional Autónoma de México, Priv. Xochicalco s/n Col. Centro, Temixco Morelos, México

[2]Building Physics and Services, Eindhoven University of Technology, P.O. Box 513, 5600 MB Eindhoven, The Netherlands

[3]Building Physics Section, Department of Civil Engineering, Leuven University, Kasteelpark Arenberg 40 bus 2447, 3001 Heverlee, Belgium

Corresponding author: J. A. Castillo, jacat@ier.unam.mx

Abstract

Natural ventilation is an alternative to create comfortable and healthy indoor conditions. This work presents the development of a method, named, the Heat Balance Index, HBI. This new index evaluates the occupant thermal comfort produced by natural ventilation in hot climates. It is based on the Heat Stress Index, HSI, model. The HBI gives the comfort velocity range, which is useful to calculate the well-ventilated percentage of a space. The numerical simulation of the cross ventilated building using Computational Fluid Dynamics was validated with experimental results. Numerical simulation of a cross ventilated building is used as an application example.

1 Introduction

Natural ventilation is an alternative to create comfort and healthy indoor conditions, reducing the energy consumption, for ventilation in general and in hot climates also for improving hygrothermal comfort. Typically, the energy cost of a naturally ventilated building is 40% less than that of an air-conditioned building (Energy Efficiency Best Practice Programme (EEBPP), 1993). For dry hot climates, it has been found that night ventilation is an effective method to promote thermal comfort conditions (Bleem et al., 1987), while for humid hot climates full day ventilation is the better strategy to promote thermal comfort conditions (Liping and Hien, 2007). Thus it is important to asses the indoor natural ventilation in hot climates in terms of the thermal comfort of the occupants.

The parameters used to evaluate the ventilation performance are the mean velocity at the space, V, and the average velocity coefficient at a slice of a given height, C_{Vh} (Prianto and Depecker, 2002). Bastide et al. (2006) have introduced the concept of well-ventilated percentage of a space, P, that is defined as the percentage of the volume with velocities within a velocity range, (U_{min}, U_{max}). They show that the results are very sensitive to the choice of U_{min} and U_{max}, but they do not give a methodology to select these values.

For the evaluation of thermal comfort, the most common method is the Predicted Mean Vote, PVM, with the Predicted Percentage Dissatisfied, PPD, (Fanger, 1970; ASHRAE, 2005), however, it has been proven that the $PVM - PPD$ method is inadequate in case of natural ventilation (De Dear et al., 1997). By contrast, the Heat Stress Index, HSI (Givoni, 1969), is a method used to evaluate thermal comfort for ventilated indoors in hot climates. It is defined as the ratio of the required evaporation to the maximum evaporative capacity of the air. The required evaporation is given by the total heat stress acting on the body (metabolism $\pm$ radiation $\pm$ convection).

This work presents the development of a method, the Heat Balance Index, HBI, to evaluate the indoor natural ventilation in hot climates in terms of the thermal comfort of the occupants. This index is developed using the assumptions and starting from the Heat Stress Index model and gives a method to define the comfort velocity range (U_{min}, U_{max}) useful to calculate the well-ventilated percentage of

a space, P. As example of application, a simulation, by Computational Fluid Dynamics (CFD), of a cross ventilated building (Kurabuchi et al., 2004) was evaluated with the climate conditions of Temixco, Morelos, which is a Mexican city with hot climate.

The fundamentals of the developed methodology are presented in Section 2. Section 3 describes the study case used to show the applicability of the proposed methodology. Conclusions are given in Section 4.

2 Methodology

The Heat Balance Index, HBI, is defined as the ratio between the heat balance of the body and the metabolic gain, which depends on the activity. The heat balance of the body is given by the algebraic sum of the metabolic gain and the heat transfer between the body and the surroundings given by the mechanisms of radiation, R (W/m^2), convection, C (W/m^2), and evaporation, E (W/m^2),

$$HBI = \frac{M \pm R \pm C - E}{M}, \tag{1}$$

where M (W/m^2) is the metabolic gain. The following empirical expressions for R, C and E (McIntyre, 1980; Wang et al., 2011) are used,

$$R = 4.4\,(T_s - T_r)\,, \tag{2}$$

$$C = 4.6U^{3/5}\,(T_s - T_a)\,, \tag{3}$$

$$E = 7.0U^{3/5}\,(P_s - P_a)\,, \tag{4}$$

where $T_s = 35°C$ is the skin temperature, T_r $(°C)$ is the mean radiant temperature, U (m/s) is the air velocity, T_a $(°C)$ is the air temperature, $P_s = 56 \times 10^2 Pa$ the vapor saturation pressure at T_s and P_a $(10^2 Pa)$ is the partial pressure of water vapor at T_a. As the evaporation is only possible if $P_s > P_a$, if this condition is not fulfilled $E = 0$ in Eq. (4).

Table 1 shows the range of conditions covered by the empirical expressions (Eqs.2 -4). This range of conditions allows a proper application in hot climates, as the climate studied in this paper, which will be detailed in Section 3.

Table 1. The range of conditions covered by the HBI.

Lower limit		Upper limit
$65 W/m^2$	$\leq M \leq$	$327 W/m^2$
$21°C$	$\leq T_a \leq$	$49°C$
$0.25 m/s$	$\leq U \leq$	$10.00 m/s$
$3\times10^2 Pa$	$\leq P_a \leq$	$56\times10^2 Pa$

The HBI of 0 represents the neutral thermal condition, where the heat generated by the body (M) is exactly equal to the heat dissipated to the surroundings. For this work, the range $-0.2 \leq HBI \leq 0.2$ is considered the comfort range (Givoni, 1969; McIntyre, 1980). $HBI < -0.2$ indicates that the body has an overdissipation greater than the 20%, with respect of M, causing a cold uncomfort. On the other hand, $HBI > 0.2$ signifies that the body has a subdissipation greater than the 20%, thus the body feels a hot uncomfort.

In order to evaluate the range for thermal comfort of the magnitude of the air velocity produced by natural ventilation, U is solved from Eq. (1),

$$U = \left[\frac{M\,(1 - HBI) - R}{4.6\,(T_s - T_a) + 7.0\,(P_s - P_a)}\right]^{5/3}. \tag{5}$$

As can be observed, U depends on HBI. Three magnitudes of U are distinguished: U_{max}, U_{neu} and U_{min}, for the HBI values of -0.2, 0.0 and 0.2, respectively. Thus $U_{min} \leq U \leq U_{max}$, represents the comfort air velocity range given an activity (M) and air temperature (T_a) and relative humidity (RH). When the value of U obtained from Eq. 5 is negative, this indicates that the air is unable to dissipate the heat generated by the body. The values of U_{max}, U_{neu} and U_{min} can be used to evaluate the comfort generated by the air velocity distribution into the building interior.

3 HBI example

3.1 CFD simulation

The cross ventilation in a scaled building (1/15), studied by Kurabuchi et al. (2004), of $0.3m \times 0.3m \times 0.15m$ ($l \times b \times h$) with two axial openings (Figure 1a) was simulated using the commercial CFD code FLUENT14.0 (ANSYS, 2011). The openings have dimensions $0.06m \times 0.03m$ ($w_w \times h_w$) and were installed at the middle of each wall, leeward and windward, respectively (Figure 1b). The CFD simulation reproduces the building geometry (small scale) and uses the reference velocity, $U_{ref} = 7m/s$, measured at h (Kurabuchi et al., 2004). The wind direction is parallel to the measurement plane. The building Reynolds number is $Re = U_{ref}h/\nu = 6.69 \times 10^4$ where ν is the dynamic viscosity of the air.

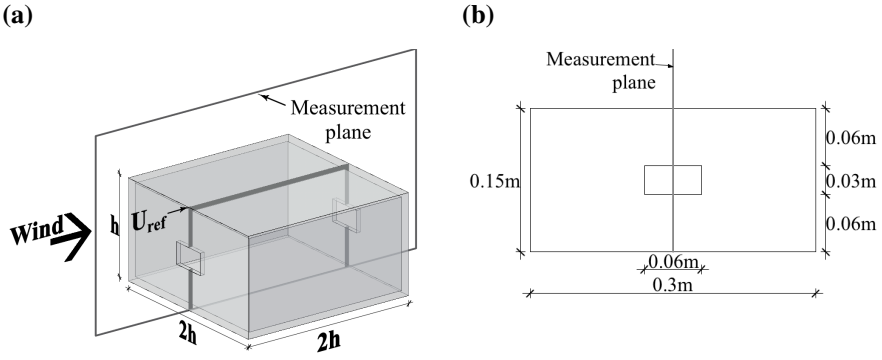

Figure 1. Scaled model of a building with two axial openings (Kurabuchi et al., 2004): (a) Right isometric view with measurement plane; (b) Front view with dimensions.

The 3D steady RANS equations were solved in combination with the shear-stress transport (SST) $k-\omega$ model (Ramponi and Blocken, 2012). The SIMPLEC algorithm was used for pressure-velocity coupling, pressure interpolation was second order and second-order discretization schemes were used for both the convection terms and the viscous terms of the governing equations. The convergence was assumed to be obtained when all the scaled residuals be less than 10^{-6}. The domain dimensions and the computational grid were based on the guidelines by Franke et al. (2007); Tominaga et al. (2008); Hooff and Blocken (2010); Ramponi and Blocken (2012), which dimensions were $W_d \times L_d \times H_d = 1.8 \times 3.0 \times 0.9m^3$ (Figure 2a). The computational base grid, formed by 1,448,712 hexahedral cells (Figure 2b), was created. The inlet boundary conditions were the wind velocity profile defined by the logarithmic law, $U(z) = (u^*_{ABL}/\kappa)ln((z+z_0)/z_0)$, with the atmospheric boundary layer (ABL) friction velocity, $u^*_{ABL} = 0.75m/s$, the von Karman constant, $\kappa = 0.42$, the roughness length, $z_0 = 0.0027m$, and the height coordinate, z. The turbulent kinetic energy (TKE) profile, $k(z) \cong \sigma^2_u(z)$, was obtained from the standard deviation of velocity in the x-direction, σ_u. The turbulence dissipation rate (TDR) and the specific dissipation rate (SDR) profiles were calculated, $\varepsilon(z) = u^{*3}_{ABL}/\kappa(z+z_0)$ and $\omega(z) = \varepsilon(z)/C_\mu k(z)$, respectively, with the empirical constant $C_\mu = 0.09$ (Tominaga et al., 2008). The standard wall functions with roughness modification (Cebeci and Bradshaw, 1977) were imposed on the ground surface. The values of the sand-grain roughness height, $k_S = 9.793z_0/C_S = 0.0039m$, and the roughness constant, C_S, were determined by using the relationship with the aerodynamic roughness length z_0 derived by Blocken et al. (2007). The standard wall functions were also used at the building surfaces, but with zero roughness height ($k_S = 0$). At the outlet plane, the zero static pressure was applied. Symmetry conditions were applied at the top and the lateral sides of the domain.

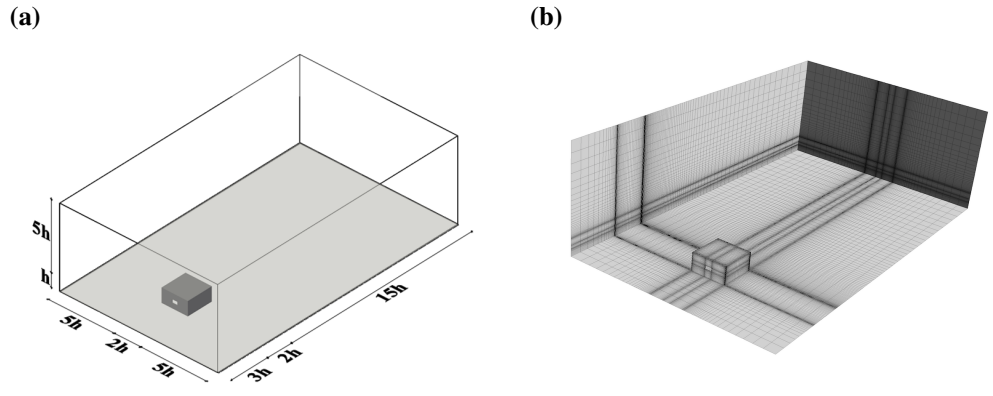

Figure 2. Computational domain with the building with two axial openings: (a) Perspective view with dimensions of the domain; (b) Perspective view of grid at bottom, side and back face (Base grid with 1,448,712 cells).

Figure 3 shows the velocity profile at inlet and at incident building position, which are an important quality criterion for the simulations (Blocken et al., 2007), in the empty domain. The test is to assess the extent of unintended streamwise gradients of the mean wind speed and the turbulence parameters, between the vertical profiles at inlet and at incident building position. In Figure 3, the inlet vertical profile (solid line) and the incident vertical profile (dashed line) are presented. Minor streamwise gradients are observed.

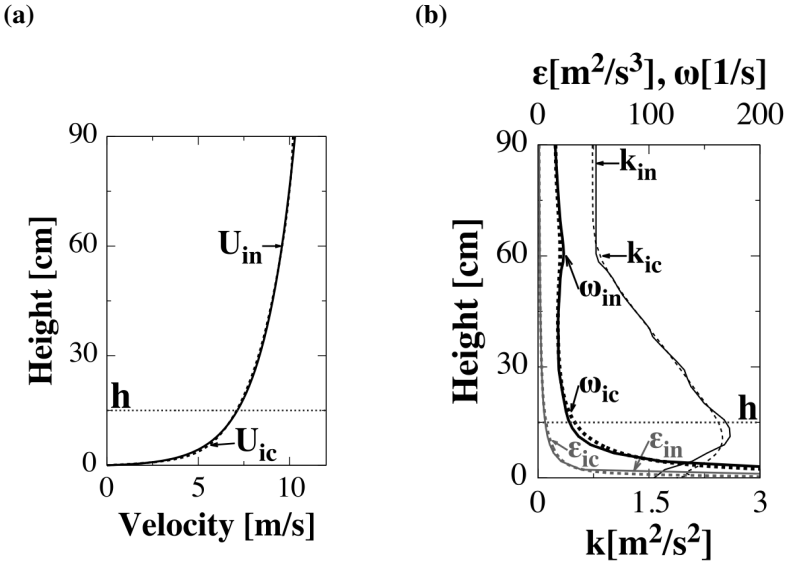

Figure 3. Vertical profiles of (left) the mean wind speed, U; (right) the turbulent kinetic energy (thin line), k, the turbulence dissipation rate (thick line), ε, and the specific dissipation rate (gray line), ω, at the inlet (solid line) and at the incident position (dashed line) in the empty domain. The subscripts "in" and "ic" refer to inlet and incident, respectively. The height of the model (h) is 0.15 m (SST $k-\omega$ model, Base grid with 1,448,712 cells).

Three grids with 728,724 cells (Coarse grid), 1,448,712 cells (Base grid) and 2,537,020 cells (Fine grid) were constructed (Figure 4). The grids were obtained by refining the Coarse grid twice by a factor of 2.

The vector field in the centerplane shows a close qualitative agreement between experimental and numerical results (Figures 5a and 5b). The simulation reproduces the main vortexes of the flow, such as the one formed by the floor and the windward wall, the one formed by the roof and the windward wall, and the biggest one in the rear of the building. The simulation tends to overestimate the structure size of the external vortexes round the scaled building. Besides, at interior of scaled building the simulation

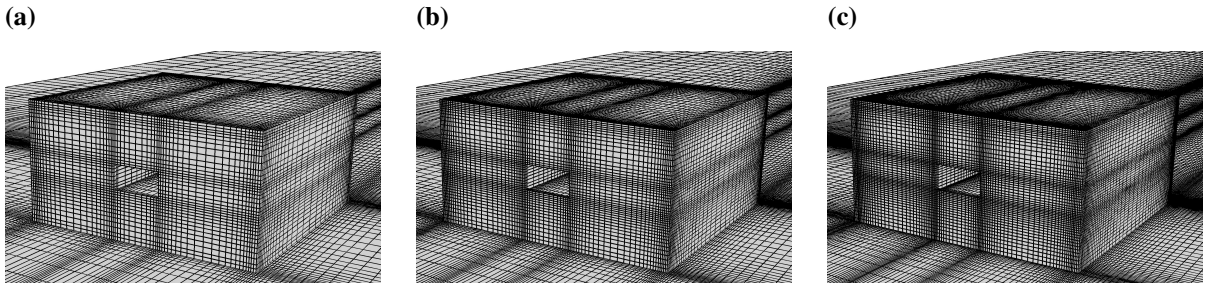

Figure 4. Isometric view of a building with two axial openings: (a) Coarse grid with 728,724 cells; (b) Base grid with 1,448,712 cells; (c) Fine grid with 2,537,020 cells.

reduces the wind speed magnitude and the size of the structures. In Figure 5c, the grid sensitivity is small along the center line, L_r. The difference of the wind speed ratio, u/U_{ref}, between the Coarse grid and Base grid at the building interior is around 7%, while between the Base grid and the Fine grid is lower than 2%. The percentage average difference between the experimental, PIV, and the numerical results, CFD, of the wind speed, $\Delta u = (PIV - CFD/U_{ref}) * 100$, along L_r is for the Base grid 6% at the interior building. Therefore, the Base grid is a suitable grid to use. Thus the validated numerical simulation of a building with two axial openings is used for the application example of the HBI.

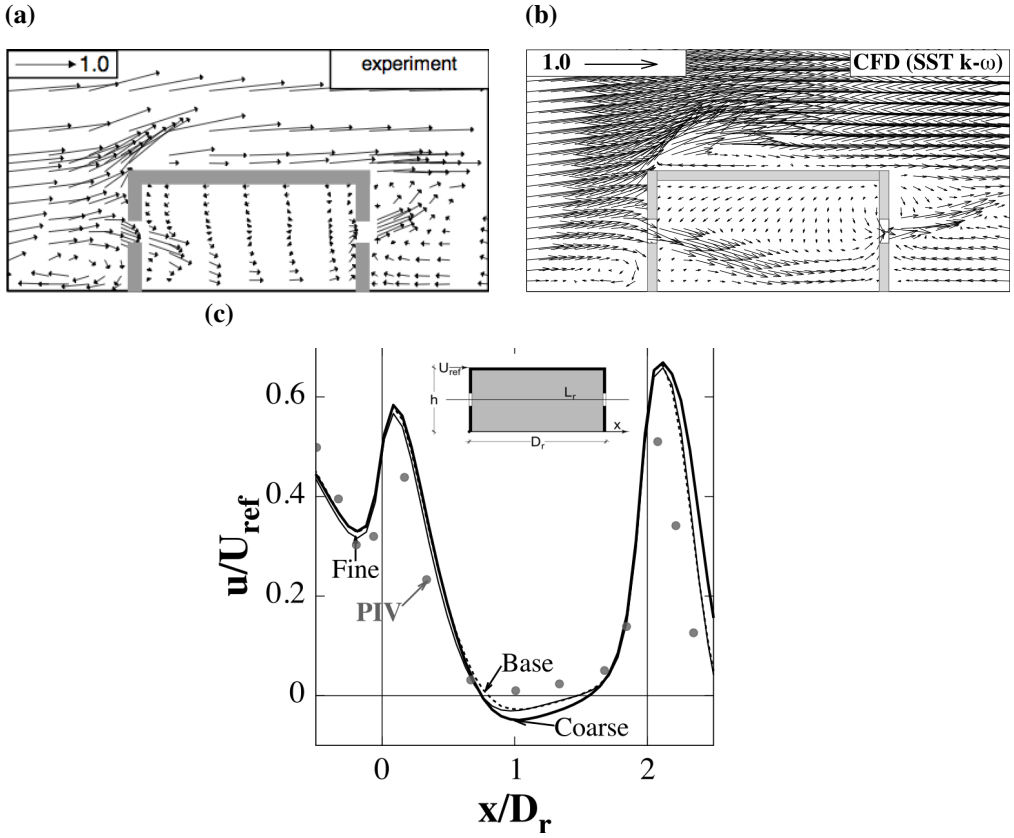

Figure 5. Comparison of mean wind vectors on the vertical centreplane and of wind speed ratio, u/U_{ref}, along the center line, L_r. (a) Experimental results from Kurabuchi et al. (2004), (b) simulation results using CFD SST $k-\omega$ turbulence model and (c) grid sensitivity analisys.

3.2 Application example

The HBI application example is performed with the climate conditions of the hot and humid season in the Temixco city located in Morelos, Mexico. The average conditions are $U_r = 1.04m/s$ (the reference

air velocity at $H_r = 2.25m$ building height), $T_r = T_a = 33°C$ and $RH = 72\%$. The $U(z)$ from the real scale were modeled as inlet boundary condition, in the validated numerical model, by applying the dynamic similarity with $Re_r = (U_r H_r)/\nu = 1.49 \times 10^5$. For thermal comfort evaluation by natural ventilation, the interior volume simulated was discretized in 4000 cells. Then, the U values obtained from each cell were scaled to real scale by using Re_r. Figure 6 shows the comfort evaluation by natural ventilation of the building with cross ventilation (Figure 1), applying Eq. (5) and considering a Metabolic rate of $M = 93W/m^2$ (light activity). Therefore, the interior volume can be zoned as: discomfort by low ventilation, D_{lv}, comfort, C_m, and discomfort by high ventilation, D_{hv}, represented by 85.8%, 12.6% and 1.7%, respectively.

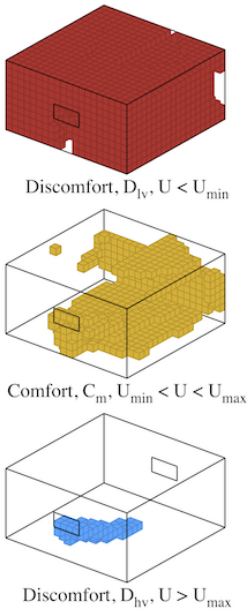

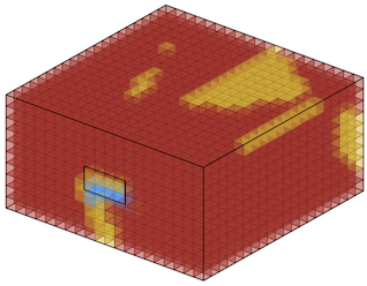

Volume	Cells	Percentage
D_{lv}	3430	85.8
C_m	504	12.6
D_{hv}	66	1.7
Total	4000	100.0

Figure 6. Evaluation of the comfort by natural ventilation of a building with cross ventilation. The interior volume is zoned as: discomfort by low ventilation, D_{lv}, comfort, C_m, and discomfort by high ventilation, D_{hv}. The range $U_{min} \leq U \leq U_{max}$ refers to the comfort air velocity range.

4 Conclusions

A methodology to evaluate the indoor comfort by natural ventilation in hot climates based on a heat balance index has been proposed. The methodology allows to evaluate CFD simulations as well as measurements taken from experiments (small or real scale). More research is needed to further verify the applicability of this methodology to select the best natural ventilation strategy.

Acknowledgements

The partial economic support from PAPIIT-UNAM IN113314 project is acknowledged. J.A. Castillo acknowledge the scholarship given by CONACYT. The authors also wish to express their gratitude to the Eindhoven University of Technology for providing the computational facilities.

References

ANSYS (2011). *ANSYS FLUENT user's guide*. ANSYS Inc, Pennsylvania.

ASHRAE (2005). *2005 ASHRAE Handbook fundamentals, Si Edition*. American Society of Heating, Refrigerating and Air Conditioning Engineers, Atlanta, GA.

Bastide, A., Lauret, P., Garde, F., and Boyer, H. (2006). Building energy efficiency and thermal comfort in tropical climates. Presentation of a numerical approach for predicting the percentage of well-ventilated living spaces in buildings using natural ventilation. *Energy and Buildings* **38**.9, pp. 1093–1103.

Bleem, J., Burns, P., and Winn, C. B. (1987). NIGHT VENTILATION STRATEGIES IN DRY CLIMATES. *Solar Engineering*. Vol. 2, pp. 959–966.

Blocken, B., Stathopoulos, T., and Carmeliet, J. (2007). CFD simulation of the atmospheric boundary layer: wall function problems. *Atmospheric Enviroment* **41**, pp. 238–252.

Cebeci, T. and Bradshaw, P. (1977). *Momentum transfer in boundary layers*. New York: Hemisphere Publishing Corp.

De Dear, R.J., Brager, G.S., and Cooper, D. (1997). *Developing an adaptive model of thermal comfort and preference, ASHRAE RP-884 Final report, ASHRAE Inc. and Macquarie Research Ltd., Sydney MRL.*

Energy Efficiency Best Practice Programme (EEBPP) (1993). *Energy Consumption Guide 19, Energy Efficiency in Offices, Energy Efficiency Office/HMSO, London.*

Fanger, P.O. (1970). *Thermal Comfort Analysis and Applications in Environmental Engineering*. New York: EngineersMcGraw-Hill.

Franke, J., Hellsten, A., Schlunzen, H., and Carissimo, B. (2007). Best practice guideline for the CFD simulation of flows in the urban environment. *COST office*.

Givoni, B. (1969). *Man, Climate and Architecture. Elsevier Architechtural Science Series*. Elsevier, Amsterdam - London - New York.

Hooff, T. van and Blocken, B. (2010). Coupled urban wind flow and indoor natural ventilation modelling on a high-resolution grid: a case study for the Amsterdam Arena stadium. *Environ Modell Softw* **25**, pp. 51–65.

Kurabuchi, Takashi, Ohba, Masaaki, Endo, Tomoyuki, Akamine, Yoshihiko, and Nakayama, Fumihiro (2004). Local Dynamic Similarity Model of Cross-Ventilation Part 1 - Theoretical Framework. *International Journal of Ventilation* **2**.4, pp. 371–382.

Liping, W. and Hien, W. N. (2007). The impacts of ventilation strategies and facade on indoor thermal environment for naturally ventilated residential buildings in Singapore. *Building and Environment* **42**.12, pp. 4006–4015.

McIntyre, D. A. (1980). *Indoor Climate*. Applied Science Publishers LTD, London, UK.

Prianto, E. and Depecker, P. (2002). Characteristic of airflow as the effect of balcony, opening design and internal division on indoor velocity: A case study of traditional dwelling in urban living quarter in tropical humid region. *Energy and Buildings* **34**.4, pp. 401–409.

Ramponi, R. and Blocken, B. (2012). CFD simulation of cross-ventilation for a generic isolated building: Impact of computational parameters. *Building and Environment* **53**, pp. 34–48.

Tominaga, Y., Mochida, A., Yoshie, R., Kataoka, H., Nozu, T., and Yoshikaw, M. (2008). AIJ guidelines for practical applications of CFD to pedestrian wind environment around buildings. *J Wind Eng Ind Aerodyn* **96**, pp. 1749–1761.

Wang, L., Liu, J., Liu, Y., Wang, Y., and Chen, J. (2011). Study on thermal environment of traditional architecture in tropic climate. *Advanced Materials Research*, pp. 6857–6861.